Observational Evidence for Summer Rainfall at Titan's North Pole

Rajani D. Dhingra[1] , Jason W. Barnes[1], Robert H. Brown[2], Bonnie J. Burrati[3], Christophe Sotin[3], Phillip D. Nicholson[4], Kevin H. Baines[5] , Roger N. Clark[6], Jason M. Soderblom[7] , Ralf Jauman[8], Sebastien Rodriguez[9] , Stéphane Le Mouélic[1,10] , Elizabeth P. Turtle[1,11] , Jason E. Perry[1,2,12] , Valeria Cottini[1,3,13], and Don E. Jennings[1,4,14]

[1]Department of Physics, University of Idaho, Moscow, ID, USA, [2]Department of Planetary Sciences, University of Arizona, TucsonAZ, USA, [3]Jet Propulsion Laboratory, Caltech, Pasadena, CA, USA, [4]Astronomy Department, Cornell University, Ithaca, NY, USA, [5]Space Science and Engineering Center, University of Wisconsin-Madison, Madison, WI, USA, [6]Planetary Science Institute, Tucson, AZ, USA, [7]Department of Earth, Atmospheric and Planetary Sciences, Massachusetts Institute of Technology, Cambridge, MA, USA, [8]Deutsches Zentrum fr Luft- und Raumfahrt, Cologne, Germany, [9]Institut de Physique du Globe de Paris, Paris, France, [10]Laboratoire de Planetologie et Geodynamique, CNRS UMR6112, Universite de Nantes, Nantes, France, [11]Johns Hopkins Applied Physics Laboratory, Laurel, MD, USA, [12]Lunar and Planetary Laboratory,University of Arizona, Tucson, AZ, USA, [13]Department of Astronomy,University of Maryland, College Park, MD, USA, [14]Goddard Space Flight Center, Greenbelt, MD, USA

Abstract Methane rain on Saturn's moon Titan makes it the only place, other than Earth, where rain interacts with the surface. When and where that rain wets the surface changes seasonally in ways that remain poorly understood. Here we report the discovery of a bright ephemeral feature covering an area of 120,000 km^2 near Titan's north pole in observations from *Cassini's* near-infrared instrument, Visual and Infrared Mapping Spectrometer on 7 June 2016. Based on the overall brightness, spectral characteristics, and geologic context, we attribute this new feature to specular reflections from a rain-wetted solid surface like those off of a sunlit wet sidewalk. The reported observation is the first documented rainfall event at Titan's north pole and heralds the arrival of the northern summer (through climatic evidence), which has been delayed relative to model predictions. This detection helps constrain Titan's seasonal change and shows that the "wet-sidewalk effect can be used to identify other rain events."

Plain Language Summary Cassini arrived in the Saturnian system in the southern summers of 2004. As expected, the Cassini team observed cloud cover, storms, and precipitation on the south pole. Like Earth, Titan has an axial tilt (27°) and its seasons vary over its year (30 Earth years). Ever since this shift in season began, the Cassini team eagerly waited for observations indicating cloud cover and precipitation that went missing from the northern latitudes. Our rainfall observation at the north pole is a major finding for two important reasons. First, this discovery observation heralds the much awaited arrival of the north polar summer rainstorms on Titan. This atmospheric phenomenon has been delayed compared to the theoretical predictions and was perplexing Titan researchers and climate modelers especially because the north pole hosts most of Titan's lakes and seas. Second, it is extremely difficult to detect rainfall events on Titan due to its thick atmospheric haze and very limited opportunities to view the surface (and its changes). We have used a novel phenomenon—the smoothening of a previously dry, rough surface by a thin layer of fluid after rainfall, similar to a wet sidewalk—as evidence for rainfall events on the surface of Titan.

1. Introduction

A major objective of the *Cassini* Solstice Mission was to search for evidence of seasonal changes on Titan (Ádámkovics et al., 2007; Tokano et al., 2006)—both atmospheric (clouds) and surficial (rainfall)—that were expected to occur as Titan moved toward the northern summer solstice in 2017. Cassini arrived in the Saturn system during southern summer (2004) and observed clouds and rainfall at the south pole (Porco et al., 2005; Schaller, Brown, Roe & Bouchez 2006; Turtle et al., 2009), consistent with general circulation models (GCMs; Schneider et al., 2012; Tokano & Lorenz, 2006). However, as northern summer approached, the increase in cloud activity in the northern hemisphere that was predicted by such models was not observed. In particular, models predicted an increase in the cloud, storm, and rain activity by 2016. Instead, only small, isolated patches of clouds over the north pole began appearing in 2014 (T104 and later flybys).
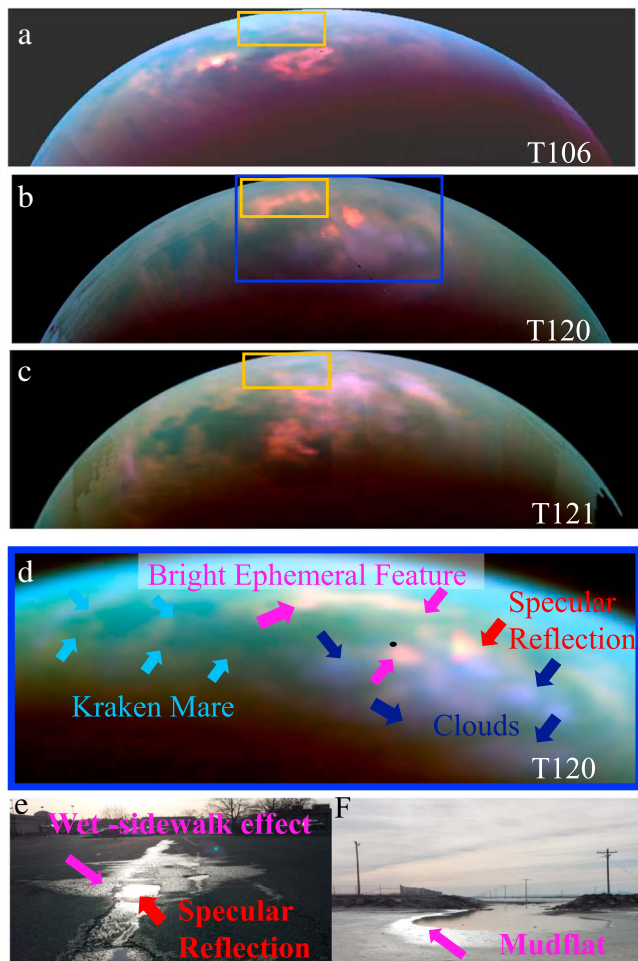
Figure 1. Visual and Infrared Mapping Spectrometer wet-sidewalk color composite (R: 5 μm, G: 2.7 μm, B: 2 μm) of Titan's north polar region showing the region corresponding to the bright ephemeral feature (BEF) in the flybys (a) T106, 24 October 2014 (b) T120, 7 June 2016, and (c) T121, 25 July 2016. The yellow box in c shows the disappearance of the BEF 3 Titan days later (see Table 1). (d) Zoomed-in view of the north polar region from the T120 flyby annotated to identify the features. The BEF is marked by magenta arrows in the figure. The black dot marks the north pole. (e) Analog for the T120 BEF on a cloudy day after rainfall. The specular reflection at the boundary of a puddle can be seen as a bright speck, while the road's wetted surface is reflecting broadly at the right geometries. (f) Analog for the T120 BEF as mudflat in Utah's Bonneville salt flats.

While both Cassini and Earth-based telescopes (Roe et al., 2002; Schaller, Brown, Roe, Bouchez, & Trujillo, 2006) have observed clouds on Titan, rain has only been inferred through observed surface changes that require high resolution views. Although four instruments on Cassini were able to observe Titan's surface: the RADAR (Elachi et al., 2004), Imaging Science Subsystem (ISS; Porco et al., 2004), Visual and Infrared Mapping Spectrometer (VIMS; Brown et al., 2004), and Composite Infrared Spectrometer (CIRS; Jennings et al., 2017), only the VIMS and ISS instruments operate at short-enough wavelengths to observe surficial veneers like rainfall.

The ISS instrument observed Titan's surface through the CB3 filter at 0.93 μm and detected surface darkenings associated with rainfall events at southern high latitudes near the beginning of the mission (southern summer; Turtle et al., 2009) and later at equatorial latitudes close to the spring equinox (Turtle et al., 2011). Subsequent to each of these events, VIMS observed surface brightening over months to years after the presumed rainfall (Barnes, Buratti, et al., 2013). In neither case could VIMS detect the initial darkening of the surface (likely due to timing and flyby geometries). CIRS in the past has detected seasonal changes in surface temperature variations (Cottini et al., 2012).

2. Observation

Herein, we report the discovery of an extensive ephemeral feature (Figure 1) near Titan's north pole that was observed by Cassini VIMS during the T120 (7 June 2016) flyby and which had disappeared by the next flyby, T121 (25 July 2016, with similar observation geometry); 3 Titan days (48 Earth days) later. The ephemeral feature is distinct due to its brightness, especially at longer wavelengths (5 μm) and covers an area of ~120,000 km² (spreading across 12 VIMS pixels; bigger than any of the Great Lakes on Earth). The spatial sampling of these pixels is on average ~130 km in the north-south direction and ~50 km in the east-west direction. In addition to the spectral data from VIMS, we use data from the RADAR, ISS, and CIRS instruments to constrain the origin and nature of this anomalously bright, ephemeral feature that we henceforth call the *bright ephemeral feature* (BEF). The ISS and VIMS data provide spectral information, RADAR data provide geologic context, while the CIRS data provide insight into the regional temperatures.

The previous flyby, T119 (6 May 2016), occurred 2 Titan days before the T120 flyby, and showed cloud cover over the north pole in VIMS data (see SOM for an image of T119). Prior to this, the region had most recently been observed by VIMS during the T106 flyby ~2 years earlier (24 October 2014), and the BEF was not observed (Figure 1a; see SOM for observation geometries). The ephemeral nature of the feature suggests that the BEF was formed by some transient, short-lived process at the north polar region of Titan, which distinctly brightened the region during T120 flyby. Later, the region resumed its usual spectral characteristics by the next flyby, T121 (Figure 1c). We propose that the BEF represents a broad specular reflection from a wetted surface brought about by rainfall.

3. Method

To study how quickly the BEF changed, we compared the region corresponding to the BEF in the T120 flyby with the next flyby, T121, and the prior flyby in which the region was visible, T106. Table 1 shows the observation geometries of the VIMS data cubes used. To rule out the possibility that we did not observe the BEF in T106 and T121 due to unfavorable geometry, we list the distance of the T120 BEF from the specular point in each flyby in Table 1. The distance of BEF from the inferred specular point for T106 and T121 (847

Table 1
Details of T106, T120 and T121 Flybys, Which Cover the Location of BEF Over Three Time Stamps

| Flyby info	Cube number	Pixel sampling (pixels per degree)	Phase (°)	Incidence (°)	Emission (°)	Inferred sp. pt.	Distance from BEF (km)	Spatial sampling (lat × long) (kilometers per pixel)
T106, 24 October 2014	CM1792831393	2.2	120	50	73	71° N, 65° W	847	100 × 90
T120, 7 June 2016	CM1844022476	2.08	116	52	65	82° N, 78° W	632	55 × 70
T121, 25 July 2016	CM1848148220	3.1	113	65	55	83° N, 6° W	470	55 × 35

Note. It helps us determine the existence of this feature over time, and we conclude that it is an ephemeral feature. The inferred specular points of the flybys are tabulated. We also show the distance of T106 and T121 specular points from the BEF; sp. pt. means specular point. The fact that the distance of inferred specular point. BEF = bright ephemeral feature.

and 470 km) is marginally different from T120's (632 km). Given the small change in the distance between the BEF and T106, T121 specular points, we would have observed the feature if BEF was present on T106 and T121 flybys. This indicates that we do not see the feature in T106 and T121 flyby due to its ephemerality rather than observation geometry.

We create a VIMS color composite of the observation and overlay it on the RADAR map of the north pole of Titan to infer the geographic location of the BEF in Figure 2. We then create spectra of different spectroscopic units and compare their brightnesses in Figure 3.

When we compare the spectra of different units from the T120 observation in Figure 3b, namely, BEF, specular, clouds, evaporite, and land, we use spectra from the same cube to minimize the atmospheric effects due to observation geometry (see SOM).

The areas where we see the BEF in VIMS are observed at high phase and emission angles by ISS (at 0.93 μm), which makes it difficult for ISS to detect any darkening or brightening associated with the region. CIRS
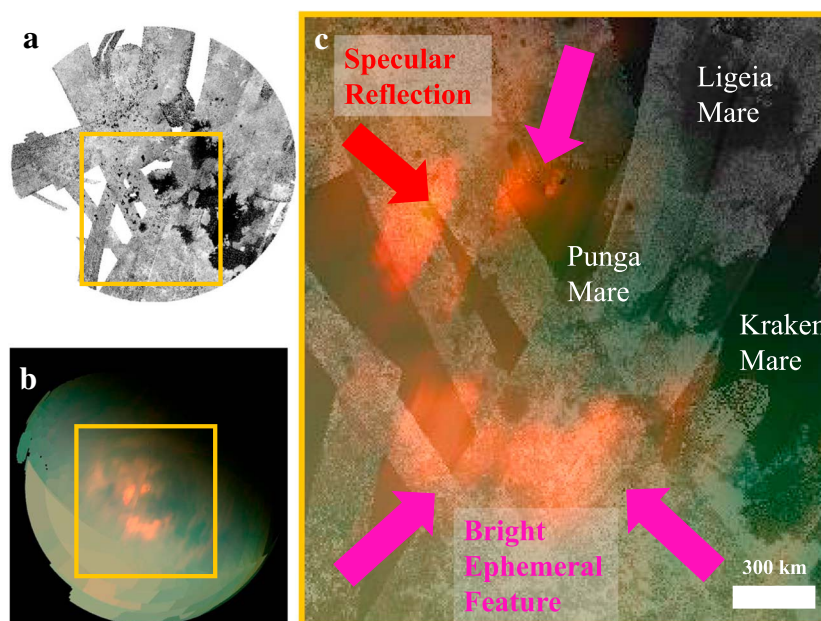
Figure 2. The figure is in a different orientation than Figure 1. Kraken Mare is in the bottom right as opposed to the bottom left in the previous figures. (a) RADAR map of the north polar region of Titan in Polar Stereographic projection. The yellow box indicates the region corresponding to the bright ephemeral feature (BEF) illustrating that the region is mostly solid land. The non-data regions are white. (b) Visual and Infrared Mapping Spectrometer infrared color composite (R: 5 μm, G: 2.7 μm, B: 1.3 μm) representing the yellow-boxed region as in the RADAR map of the north pole. (c) Visual and Infrared Mapping Spectrometer infrared color composite (b; R: 5 μm, G: 2.7 μm, B: 1.3 μm) overlain on the north polar map of RADAR (a) showing the BEF and specular point. The red arrow indicates the specular reflection point (82.7° N, 78.6° W) near Xolotlan Lacus. The magenta arrows indicate the BEF we observe in T120.
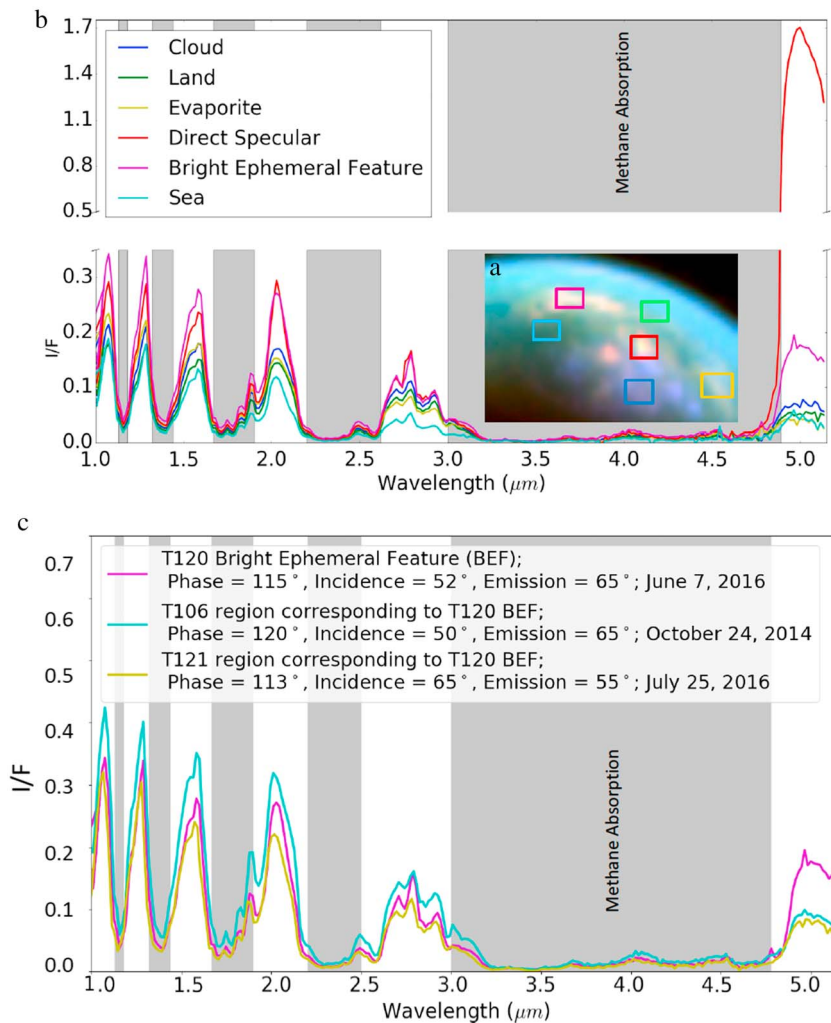
Figure 3. (a) The colored boxes correspond to the different regions in the T120 observations: dark blue (clouds), green (land), light blue (sea), red (specular reflection), magenta (bright ephemeral feature, BEF), and yellow (evaporites). (b) The spectra corresponding to the regions in similar colors as the boxes in a. Gray solid boxes show spectral regions affected by methane absorption and thus blocked by Titan's atmosphere. (c) The spectra for the location of the BEF. The slightly higher reflectance at shorter wavelengths of the T106 observation (cyan) is because of the higher emission angles. The magenta spectrum corresponds to the BEF during the T120 June 2016 flyby, which is distinctly brighter than other spectra at 5 μm. The yellow spectrum indicates reflectances for the same region 3 Titan days later during the T121 July 2016 flyby.

observations of the region, before and during/after the rainfall event, do not provide clear indications of a temperature drop due to any rainfall-derived cooling of the region.

4. Hypotheses

Several mechanisms could potentially produce the reported spectral signature in VIMS data: clouds, fog, evaporites, direct specular reflections (i.e., reflections off large smooth surfaces), and broad specular reflections. In the following text, we consider the merits of each of these possibilities and demonstrate how all but the broad specular reflections can be ruled out.

The T120 flyby contains extensive clouds in addition to the BEF that serve as the basis for our spectral comparison. Although VIMS observes from 0.3 to 5.1 μm in 352 spectral channels, Titan's surface is only visible through the atmosphere in seven narrow spectral windows, at 0.92, 1.06, 1.26, 1.57, 2.0, 2.7, and 5 μm (Brown et al., 2004). VIMS data are expressed in terms of surface reflectance as I/F (where I is the observed radiance and πF is the incident solar irradiance). The surface and clouds on Titan show distinct spectral

responses (Rodriguez et al., 2009, 2006). We incorporate these spectral response characteristics into a color composite (RGB = 5, 2, and 2.7 μm; Barnes et al., 2007; Sotin et al., 2012) to facilitate the identification of various spectral units in the observation. Though also bright at 5 μm, clouds are brighter at 2.7 μm (Griffith et al., 2009; McCord et al., 2006; Rodriguez et al., 2011) owing to their high altitude. The wings of the 2-μm band of clouds also indicate altitude. As a result, the color composite effectively distinguishes clouds (purple in Figure 1d) from BEF (orange in Figure 1d).

Low-lying clouds or fog (Brown et al., 2009), however, cannot be entirely ruled out simply based on spectral comparison of the BEF with typical high-altitude clouds. Near-surface fog is difficult to distinguish from bright surface features in spectra without a reliable atmospheric radiative transfer correction. However, both the bright and red (5 μm) spectrum of the BEF (in Titan's atmospheric windows) and the fact that the BEF does not extend over nearby large lakes (where one might expect the humidity to be higher) argues against the possibility of a low-lying fog. Even if the latter case is true, the occurrence of a fog layer necessitates a wet (humid) source underneath. Thus, the wetting of land surface by rain is strongly supported, especially considering the large areal spread of the BEF.

Evaporites, direct specular reflections, and broad specular reflections are all surface phenomena. While broad specular reflections from a liquid surface can occur if the surface is roughened by waves (Barnes et al., 2014) or nitrogen bubbles (Hofgartner et al., 2014; Malaska et al., 2017), a broad specular return from a solid surface requires smoothing of the surface at length scales comparable to the wavelength of light, as would occur if the surface were wet (like a wet sidewalk after rainfall). RADAR and ISS data observations (Figure 2) show that the BEF occurs over a solid land surface, bordering known lakes in some places: the northwestern edge of the BEF coincides with Lagoda Lacus (equivalent radius of ~54 km). However, waves on Lagoda Lacus would be discrete, smaller than the lake area, and cannot cause the bright pixels. The BEF is ~3 orders of magnitude larger than the lake.

A commonly observed unit, particularly in the north, are 5-μm bright deposits observed to abut many filled and empty lakes that are believed to be evaporitic material, comprising deposits left behind when lakes evaporate (Figure 3b; Barnes et al., 2011; MacKenzie et al., 2014). Two lines of logic, however, strongly disfavor evaporite deposits for the BEF. The first is the spatial extent. Evaporites typically only border the edges of lake—the deposit observed along the southern end of Ladoga Lacus spans an area of 300 km^2 (as observed during the T76 flyby, 8 May 2011) compared to the BEF, spanning an area of ~120,000 km^2. Second, and most importantly, no evaporites have been observed to form and then disappear within a window of only a few Titan days, as was observed for the BEF (Figures 1a–1c).

Direct specular reflections, which we define as the reflection of light off a surface that is smooth at scales both comparable to the wavelength of light and to the projected image of the Sun on the surface (Barnes, Clark, et al., 2013; Soderblom et al., 2012; Stephan et al., 2010), depend on viewing geometry and result in an unusually high I/F. In the T120 flyby we observe the direct specular reflection from the Sun (I/F of ~2 in the 5-μm spectral window) from the surface of Xolotlan Lacus at 82.7° N, 78.6° W.

We observe the direct specular reflection of the Sun (I/F of ~2 in the 5-μm spectral window) in the T120 flyby, at 82.7° N, 78.6° W from the surface of the lake, Xolotlan Lacus (Figure 2c), ~632 km away from the BEF. As a sidenote, the specular point seems close to the BEF or wet sidewalk in the Earth analog (Figure 1e). This is due to the smaller angular distance between the specular point and the BEF as compared to T120 observation.

Even though the BEF does not occur at the specular point, it does show spectral similarities to direct specular reflections on Titan. We compare the spectrum of the BEF with those of sea, clouds, land, evaporites, and the direct specular reflection (Figures 3a and 3b), all taken from the same flyby (T120) to minimize atmospheric effects (see section 3 for observation geometry). The direct specular reflection is the brightest "feature" at 5 μm in the observation. The next brightest feature at 5 μm (by 50%) is the BEF. A rough surface cannot, on its own, reflect specularly. However, surface wetting coats the irregular surfaces of the rough region resulting in a smoother surface than what is underneath. The spectral brightness and observation geometry immediately indicate that the BEF is a broad specular reflection due to smoothing of a surface that was otherwise dry.
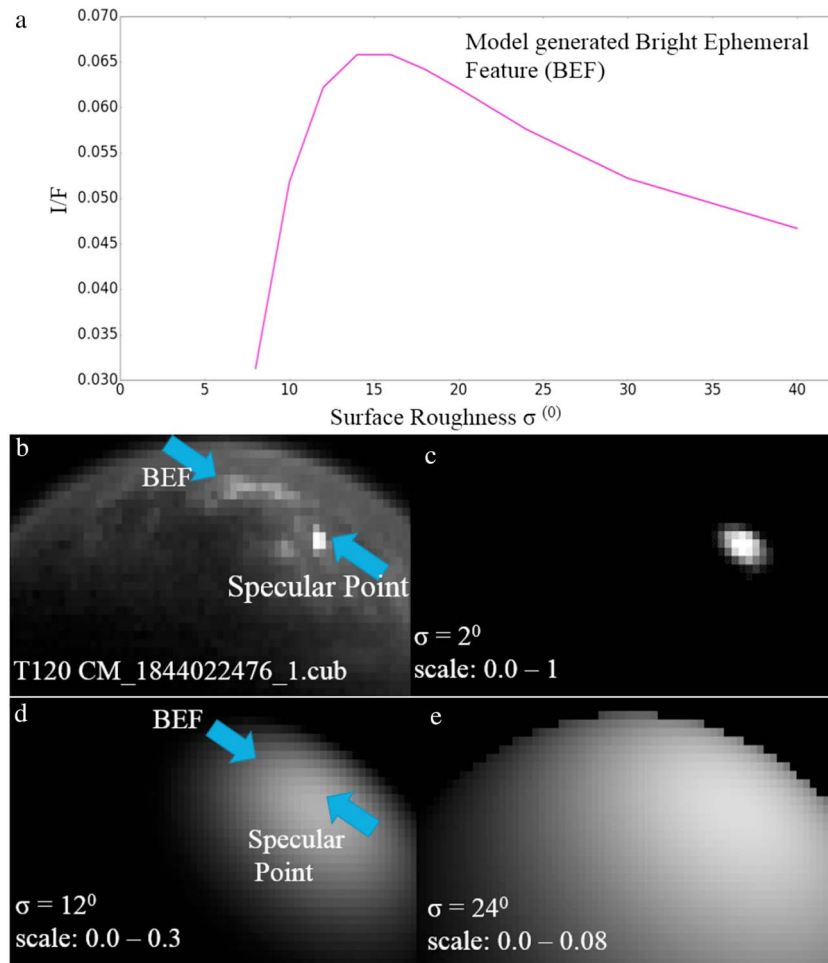
Figure 4. (a) Modeled reflectance (I/F) variation with surface roughness for the broad specular reflection (BEF) observed during the T120 flyby. The modeled (magenta) reflectance peaks at roughness (σ) values of $\sim 14°$ indicating that the BEF's surface roughness could be of that order. (b) T120 Cassini image cube CM1866022476 where the BEF is observed. (c) Model-generated synthetic images for the T120 observation geometry with a surface roughness parameter of 2° reveals only the specular reflection. One thing to note is the scale in the synthetic images: As we increase the roughness or specular deviation angle, σ, the specular reflection spreads over a larger number of pixels, each pixel receiving lesser solar flux for higher σ, and hence, the scale changes. (d) σ of 12° covers the extent of BEF. (e) σ of 24° distributes the entire solar flux onto the Titan hemisphere.

5. Modeling Surface Roughness

In order to test our hypothesis, we model the BEF's surface roughness to characterize specular reflections from a macroscopically rough surface (Figure 4). We use a numerical planetary specular model (Barnes et al., 2014; Soderblom et al., 2012) with Gaussian-distributed slopes and azimuthal symmetry, for the same observation geometry as the T120 observation (Figure 4b).

For small roughnesses with RMS slopes of $\sigma \sim 2°$ (Figure 4c), only the direct specular reflection at the specular point appears. As we increase the roughness parameter, σ, the specular reflection spreads over a larger number of pixels, each pixel receiving lesser solar flux, resulting in a fuzzier reflection distributed over a broader region. Over an area equivalent to the BEF, the model-determined σ values indicate that the required slopes to get signals comparable to our observation are $\sim 12–14°$ (Figure 4d). This is twice the σ value of the inferred waves in Punga Mare (liquid surface), which were determined using the same model, to be $\sim 6°$. Figure 4e shows that, at higher slopes, ($\sim 24°$) the reflections become independent of the roughness parameter and show the entire solar flux (I/F_{max}, see section 3) distributed over Titan's hemisphere.

6. Results and Discussion

Based on our detailed analysis of the Cassini data coupled with roughness modeling and testing the feasibility of various possibilities, we propose that the BEF represents a broad specular reflection from a rough, wetted surface—presumably brought about by rainfall (T120 flyby, 7 June 2016), 2 Titan days after the observed cloud coverage (T119 flyby, 6 May 2016). A rough land surface could be smoothed by a recent surface wetting due to a summer-rainfall event. Earth analogs of wetted sidewalks (Figure 1e) and a mudflat (Clark et al., 2010) in Utah's Bonneville Salt Flats (Figure 1f) broadly fit the BEF profile. The RADAR data show the area to be rough, variegated, and nonuniform (at scales of ∼2 cm). A wet-sidewalk region is wet on a solid but rough substrate that at the right geometries produces broad specular reflections. These help us conclude that the BEF would have properties similar to a wet sidewalk that arises from a recently wetted, solid and rough surface on the north pole of Titan.

7. Conclusion

The reduced and delayed cloud and storm activity at Titan's north pole as opposed to the model-predicted activity suggests that our current understanding of Titan's changing seasons is incomplete. Our reported observations represent the first documented rainfall event on the north pole of Titan. We discover this rainfall based on a novel technique "wet-sidewalk effect" (broad specular reflections from a smoothened, original rough surface). Identifying the location and timing of the rainfall offers important data points for Titan GCMs, helping constrain why the northern summer cloud activity is delayed relative to predictions—especially because the north pole hosts most of Titan's lakes and seas (Hayes, 2016). Apart from helping us understand Titan's weather and long term climate, a broad specular reflection observation like this helps us derive the roughness of the solid surfaces on Titan. Surface roughness of a region holds clues to its geologic evolution and nature of surface interactions and even has implications for landing site evaluations for future missions (Turtle et al., 2017) to Titan.

References

Ádámkovics, M., Wong, M. H., Laver, C., & de Pater, I. (2007). Widespread morning drizzle on Titan. *Science*, *318*, 962–965. https://doi.org/10.1126/science.1146244

Barnes, J. W., Bow, J., Schwartz, J., Brown, R. H., Soderblom, J. M., Hayes, A. G., et al. (2011). Organic sedimentary deposits in Titan's dry lakebeds: Probable evaporite. *Icarus*, *216*, 136–140. https://doi.org/10.1016/j.icarus.2011.08.022

Barnes, J. W., Brown, R. H., Soderblom, L., Buratti, B. J., Sotin, C., Rodriguez, S., et al. (2007). Global-scale surface spectral variations on Titan seen from Cassini/VIMS. *Icarus*, *186*, 242–258. https://doi.org/10.1016/j.icarus.2006.08.021

Barnes, J. W., Buratti, B. J., Turtle, E. P., Bow, J., Dalba, P. A., Perry, J. E., et al. (2013). Precipitation-induced surface brightenings seen on Titan by Cassini VIMS and ISS. *Planetary Science*, *2*(1). https://doi.org/10.1186/2191-2521-2-1

Barnes, J. W., Clark, R. N., Sotin, C., Ádámkovics, M., Appéré, T., Rodriguez, S., et al. (2013). A transmission spectrum of Titan's north polar atmosphere from a specular reflection of the Sun. *Astrophysical Journal*, *777*(2), 161. https://doi.org/10.1088/0004-637X/777/2/161

Barnes, J. W., Sotin, C., Soderblom, J. M., Brown, R. H., Hayes, A. G., Donelan, M., et al. (2014). Cassini/VIMS observes rough surfaces on Titan's Punga Mare in specular reflection. *Planetary Science*, *3*(1), 3. https://doi.org/10.1186/s13535-014-0003-4

Brown, R. H., Baines, K. H., Bellucci, G., Bibring, J.-P., Buratti, B. J., Capaccioni, F., et al. (2004). The Cassini Visual And Infrared Mapping Spectrometer (VIMS) investigation. *Space Science Reviews*, *115*, 111–168. https://doi.org/10.1007/s11214-004-1453-x

Brown, M. E., Smith, A. L., Chen, C., & Ádámkovics, M. (2009). Discovery of fog at the south pole of Titan. *Astrophysical Journal*, *706*, L110–L113. https://doi.org/10.1088/0004-637X/706/1/L110

Clark, R. N., Curchin, J. M., Barnes, J. W., Jaumann, R., Soderblom, L., Cruikshank, D. P., et al. (2010). Detection and mapping of hydrocarbon deposits on Titan. *Journal of Geophysical Research*, *115*, E10005. https://doi.org/10.1029/2009JE003369

Cottini, V., Nixon, C. A., Jennings, D. E., de Kok, R., Teanby, N. A., Irwin, P. G. J., & Flasar, F. M. (2012). Spatial and temporal variations in Titan's surface temperatures from Cassini CIRS observations. *Planetary and Space Science*, *60*, 62–71. https://doi.org/10.1016/j.pss.2011.03.015

Elachi, C., Allison, M. D., Borgarelli, L., Encrenaz, P., Im, E., Janssen, M. A., et al. (2004). Radar: The Cassini Titan radar mapper. *Space Science Reviews*, *115*, 71–110. https://doi.org/10.1007/s11214-004-1438-9

Griffith, C. A., Penteado, P., Rodriguez, S., LeMouélic, S., Baines, K. H., Buratti, B., et al. (2009). Characterization of clouds in Titan's tropical atmosphere. *Astrophysical Journal*, *702*, L105–L109. https://doi.org/10.1088/0004-637X/702/2/L105

Hayes, A. G. (2016). The lakes and seas of Titan. *Annual Review of Earth and Planetary Sciences*, *44*(1), 57–83. https://doi.org/10.1146/annurev-earth-060115-012247

Hofgartner, J., Hayes, A. G., Lunine, J., Zebker, H, Stiles, B., Sotin, C, et al. (2014). Transient features in a Titan sea. *Nature Geoscience*, *7*, 493–496. https://doi.org/https://doi.org/10.1038/ngeo2190

Jennings, D. E., Flasar, F. M., Kunde, V. G., Nixon, C. A., Segura, M. E., Romani, P. N., et al. (2017). Composite infrared spectrometer (CIRS) on Cassini: Publisher's note. *Applied Optics*, *56*(21), 5897–5897. Retrieved from http://ao.osa.org/abstract.cfm?URI=ao-56-21-5897, https://doi.org/10.1364/AO.56.005897

MacKenzie, S. M., Barnes, J. W., Sotin, C., Soderblom, J. M., Mouélic, S. L., Rodriguez, S., et al. (2014). Evidence of Titan's climate history from evaporite distribution. *Icarus*, *243*, 191–207. Retrieved from http://www.sciencedirect.com/science/article/pii/S0019103514004370, and https://doi.org/10.1016/j.icarus.2014.08.022

Malaska, M. J., Hodyss, R., Lunine, J. I., Hayes, A. G., Hofgartner, J. D., Hollyday, G., & Lorenz, R. D. (2017). Laboratory measurements of nitrogen dissolution in Titan lake fluids. *Icarus*, *289*, 94–105. https://doi.org/10.1016/j.icarus.2017.01.033

McCord, T. B., Hansen, G. B., Buratti, B. J., Clark, R. N., Cruikshank, D. P., D'Aversa, E., et al. (2006). Composition of Titan's surface from Cassini VIMS. *Planetary and Space Science*, *54*, 1524–1539. https://doi.org/10.1016/j.pss.2006.06.007

Porco, C. C., Baker, E., Barbara, J., Beurle, K., Brahic, A., Burns, J. A., et al. (2005). Imaging of Titan from the Cassini spacecraft. *Nature*, *434*, 159–168. https://doi.org/10.1038/nature03436

Porco, C. C., West, R. A., Squyres, S., McEwen, A., Thomas, P., Murray, C. D., et al. (2004). Cassini imaging science: Instrument characteristics and anticipated scientific investigations at Saturn. *Space Science Reviews*, *115*, 363–497. https://doi.org/10.1007/s11214-004-1456-7

Rodriguez, S., Le Mouélic, S., Rannou, P., Sotin, C., Brown, R. H., Barnes, J. W., et al. (2011). Titan's cloud seasonal activity from winter to spring with Cassini/VIMS. *Icarus*, *216*, 89–110. https://doi.org/10.1016/j.icarus.2011.07.031

Rodriguez, S., Le Mouélic, S., Rannou, P., Tobie, G., Baines, K. H., Barnes, J. W., et al. (2009). Global circulation as the main source of cloud activity on Titan. *Nature*, *459*, 678–682. https://doi.org/10.1038/nature08014

Rodriguez, S., Le Mouélic, S., Sotin, C., Clénet, H., Clark, R. N., Buratti, B., et al. (2006). Cassini/VIMS hyperspectral observations of the HUYGENS landing site on Titan. *Planetary and Space Science*, *54*, 1510–1523. https://doi.org/10.1016/j.pss.2006.06.016

Roe, H. G., de Pater, I., Macintosh, B. A., & McKay, C. P. (2002). Titan's clouds from Gemini and Keck adaptive optics imaging. *Astrophysical Journal*, *581*, 1399–1406. https://doi.org/10.1086/344403

Schaller, E. L., Brown, M. E., Roe, H. G., & Bouchez, A. H. (2006). A large cloud outburst at Titan's south pole. *Icarus*, *182*(1), 224–229. https://doi.org/doi:10.1016/j.icarus.2005.12.021

Schaller, E. L., Brown, M. E., Roe, H. G., Bouchez, A. H., & Trujillo, C. A. (2006). Dissipation of Titan's south polar clouds. *Icarus*, *184*(2), 517–523. https://doi.org/10.1016/j.icarus.2006.05.025

Schneider, T., Graves, S. D. B., Schaller, E. L., & Brown, M. E. (2012). Polar methane accumulation and rainstorms on Titan from simulations of the methane cycle. *Nature*, *481*, 58–61. https://doi.org/10.1038/nature10666

Soderblom, J. M., Barnes, J. W., Soderblom, L. A., Brown, R. H., Griffith, C. A., Nicholson, P. D., et al. (2012). Modeling specular reflections from hydrocarbon lakes on Titan. *Icarus*, *220*, 744–751. https://doi.org/10.1016/j.icarus.2012.05.030

Sotin, C., Lawrence, K. J., Reinhardt, B., Barnes, J. W., Brown, R. H., Hayes, A. G., et al. (2012). Observations of Titan's northern lakes at 5 μ: Implications for the organic cycle and geology. *Icarus*, *221*, 768–786. https://doi.org/10.1016/j.icarus.2012.08.017

Stephan, K., Jaumann, R., Brown, R. H., Soderblom, J. M., Soderblom, L. A., Barnes, J. W., et al. (2010). Specular reflection on Titan: Liquids in Kraken Mare. *Geophysical Research Letters*, *37*, L7104. https://doi.org/10.1029/2009GL042312

Tokano, T., & Lorenz, R. D. (2006). GCM simulation of balloon trajectories on Titan. *Planetary and Space Science*, *54*, 685–694. https://doi.org/10.1016/j.pss.2006.04.001

Tokano, T., McKay, C. P., Neubauer, F. M., Atreya, S. K., Ferri, F., Fulchignoni, M., & Niemann, H. B. (2006). Methane drizzle on Titan. *Nature*, *442*, 432–435. https://doi.org/10.1038/nature04948

Turtle, E. P., Barnes, J. W., Trainer, M. G., Lorenz, R. D., MacKenzie, S. M., Hibbard, K. E., et al. (2017). Dragonfly: Exploring Titan's prebiotic organic chemistry and habitability. In *Lunar and planetary science conference*, *48*. The Woodlands, TX. Retrieved from https://www.hou.usra.edu/meetings/lpsc2017/pdf/1958.pdf

Turtle, E. P., Perry, J. E., Hayes, A. G., Lorenz, R. D., Barnes, J. W., McEwen, A. S., et al. (2011). Rapid and extensive surface changes near Titan's equator: Evidence of April showers. *Science*, *331*, 1414–1417. https://doi.org/10.1126/science.1201063

Turtle, E. P., Perry, J. E., McEwen, A. S., Del Genio, A. D., Barbara, J., West, R. A., et al. (2009). Cassini imaging of Titan's high-latitude lakes, clouds, and south-polar surface changes. *Geophysical Research Letters*, *36*, L2204. https://doi.org/10.1029/2008GL036186